Functional *in vivo* interactions between JNK1 and JNK2 isoforms in obesity and insulin resistance

Gürol Tuncman*, Jiro Hirosumi*, Giovanni Solinas†, Lufen Chang†, Michael Karin†‡, and Gökhan S. Hotamisligil*‡

*Department of Genetics and Complex Diseases, Harvard School of Public Health, 665 Huntington Avenue, Boston, MA 02115; and †Department of Pharmacology, Laboratory of Gene Regulation and Signal Transduction, University of California at San Diego, School of Medicine, 9800 Gilman Drive, La Jolla, CA 92093

Contributed by Michael Karin, April 28, 2006

The c-Jun N-terminal kinases (JNKs) are key regulators of inflammation and interfere with insulin action in cultured cells and whole animals. Obesity increases total JNK activity, and JNK1, but not JNK2, deficiency results in reduced adiposity and improved insulin sensitivity. Interestingly, a higher-than-normal level of JNK activation is observed in *Jnk2*$^{-/-}$ mice, particularly in the liver, indicating an interaction between the isoforms that might have masked the metabolic activity of JNK2 in isolated mutant mice. To address the role of the JNK2 isoform in metabolic homeostasis, we intercrossed *Jnk1*$^{-/-}$ and *Jnk2*$^{-/-}$ mice and examined body weight and glucose metabolism in the resulting mutant allele combinations. Among all of the viable genotypes examined, we observed only reduced body weight and increased insulin sensitivity in *Jnk1*$^{-/-}$ and *Jnk1*$^{+/-}$*Jnk2*$^{-/-}$ mice. These two groups of mice also exhibited reduced total JNK activity and cytokine expression in liver tissue compared with all other genotypes examined. These data indicate that the JNK2 isoform is also involved in metabolic regulation, but its function is not obvious when JNK1 is fully expressed because of regulatory crosstalk between the two isoforms.

diabetes | fatty liver | metabolic syndrome | inflammation | stress

Obesity and associated metabolic diseases have strong inflammatory underpinnings (1). We and others have demonstrated increased TNF-α expression in obesity, which represents an important component of the link between obesity and insulin resistance (2–4). It is now recognized that TNF-α and many other inflammatory molecules are produced during the course of obesity both in experimental models and humans, particularly in adipose tissue (1). In addition to these "adipokines," lipids and lipid mediators represent another potential mediator of both inflammatory responses and insulin resistance in obesity (5, 6). Recent evidence indicates that both adipokines and fatty acids might have common targets in regulating insulin receptor signaling and consequently modulate insulin action. One such target is serine phosphorylation of insulin receptor substrate 1 (IRS-1) (7, 8). Furthermore, both TNF-α and free fatty acids (FFA) are potent regulators of c-Jun N-terminal kinase (JNK) and IκB kinase (IKK) activity, the two critical kinases that are central to engaging these molecular targets such as IRS-1, emergence of inflammatory alterations, and inhibition of insulin action in obesity (9, 10). Inhibitors of both JNK and IKK are also effective in the treatment of experimental insulin resistance and diabetes (9, 11).

In cultured cells and whole animals, JNK activity is required for coupling inflammatory and metabolic signals (10, 12). Exposure to TNF-α or fatty acids results in suppression of insulin receptor signaling through serine phosphorylation of IRS-1, an important mechanism in the inhibition of insulin action (8, 12). JNK activity is required for this modification, and in JNK-deficient cells, TNF-α fails to induce serine phosphorylation of IRS-1 and cause insulin resistance (10, 12). It is likely that JNK activation integrates responses from many stress signals and does not simply represent a downstream target of an individual mediator or a cytokine. For example, recent studies have demonstrated endoplasmic reticulum stress as an important signal leading to JNK activation in obesity (13). Fatty acid-induced insulin resistance in adipocytes also requires the presence of TNF-α and JNK activity, and it has been proposed that it might also involve activation of SOCS3 (14, 15). Interestingly, SOCS3 regulation by fatty acids also depends on JNK activity (15). Hence, activation of JNK appears to be a key mechanism by which stress signals, whether metabolic in nature or not, are linked to insulin action.

The JNK subgroup of mitogen-activated protein kinases is encoded by three loci. *Jnk1* and *Jnk2* are ubiquitously expressed, whereas *Jnk3* is expressed mainly in heart, testis, and brain (16). Initially, the different JNK isoforms were thought to have largely redundant activities, although they may differ in their catalytic activity against various substrates (17). However, several nonredundant functions were also documented. For example, in the control of CD4$^+$ effector T cell differentiation, *Jnk1*$^{-/-}$ cells exhibit polarization toward a Th2 profile, whereas *Jnk2*$^{-/-}$ cells show a tendency to undergo Th1 polarization (18–21). Some of these differences were attributed to differential phosphorylation of the E3 ubiquitin ligase Itch by JNK1 and JNK2 isoforms (22). The preferential activation of Itch by JNK1 (23) may also explain the selective involvement of JNK1 rather than JNK2 in TNF-α-induced cell death (24). Isolated JNK1 but not JNK2 deficiency results in reduced adiposity and increased insulin sensitivity in mouse models of obesity (10). Interestingly, however, JNK2 but not JNK1 deficiency was reported to provide protection against atherosclerosis and type 1 diabetes in mice (25, 26). Because JNK isoforms can influence each other's activities (27), part of this subtype specificity might be related to the action of each JNK isoform in the relevant target tissue. Alternatively, interactions between isoforms can determine compensatory total activity in isolated JNK-deficiency models. None of the previous work in metabolic disease has addressed these issues. In this study, we performed a detailed genetic analysis of the interaction between JNK1 and JNK2 isoforms in obesity and insulin resistance and examined the potential role of the *Jnk2* locus in metabolic regulation in mice.

Results and Discussion

Tissue JNK Activity in JNK1- and JNK2-Deficient Mice. Targeted deletion of *Jnk1* in mice reduces obesity-induced JNK activity and significantly elevates systemic insulin sensitivity (10). JNK2-deficient animals, however, do not exhibit any changes in insulin sensitivity or body weight. These results suggest that obesity-induced insulin resistance is predominantly mediated by JNK1

Conflict of interest statement: No conflicts declared.

Freely available online through the PNAS open access option.

Abbreviations: JNK, c-Jun N-terminal kinase; TNFR, TNF receptor; IRS-1, insulin receptor substrate 1; MIF, migration inhibitory factor.

‡To whom correspondence may be addressed. E-mail: mkarin@ucsd.edu or ghotamis@hsph.harvard.edu.

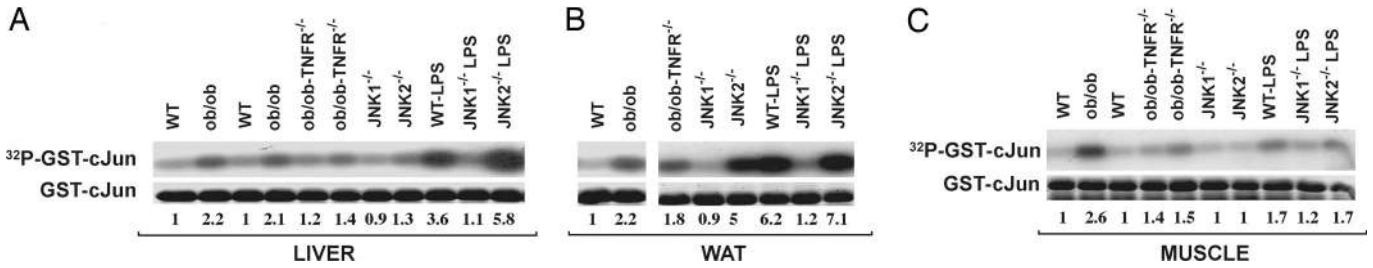

Fig. 1. Regulation of JNK activity by obesity and its modulation by isolated JNK1 and JNK2 deficiencies. Total JNK activity was determined in liver, white adipose tissue (WAT), and muscle tissues of WT, *ob/ob*, *ob/ob-TNFR*$^{-/-}$(*p55*$^{-/-}$*p75*$^{-/-}$), *Jnk1*$^{-/-}$, and *Jnk2*$^{-/-}$ mice. *ob/ob*, genetic model for leptin deficiency. Numbers below the immunoblots represent fold increase in c-Jun N-terminal phosphorylation. 1, activity in lean WT.

.

isoforms, and that JNK2 isoforms do not play a detectable role in metabolic regulation in mice. Interestingly, recent studies demonstrated that JNK2 may exert a negative regulatory effect on JNK1 (27). If this is also the case in obesity *in vivo*, then one might postulate that the lack of a visible phenotype in *Jnk2*$^{-/-}$ animals might be the result of compensatory regulation of total JNK activity, primarily through JNK1 isoforms. To address this possibility, we first examined JNK activity in liver, muscle, and fat tissues of *Jnk1*$^{-/-}$ and *Jnk2*$^{-/-}$ mice at baseline, in the presence of obesity and upon stimulation with bacterial LPS. We also examined JNK activity in obese TNF receptor (TNFR)-deficient animals (lacking both p55/TNFR1 and p75/TNFR2 in the *ob/ob* background). This latter model represents a scenario where TNF-α action through both JNK1 and JNK2 is prevented. As shown in Fig. 1, total JNK activity in obese animals was higher than lean controls in liver, muscle, and adipose tissues. Obese TNFR-deficient animals exhibited lower levels of JNK activity, but this reduction was partial, and JNK activity was still higher than in lean controls. JNK1 deficiency results in reversal of total JNK activity to baseline levels with or without obesity. Interestingly, total JNK activity in JNK2-deficient animals was consistently higher than in JNK1-deficient animals in liver and adipose tissues (Fig. 1 and data not shown). A similar pattern was also evident in the regulation of total JNK activity in *Jnk1*$^{-/-}$ and *Jnk2*$^{-/-}$ mice after LPS administration *in vivo*. In both liver and adipose tissue, LPS-stimulated JNK activity was higher in *Jnk2*$^{-/-}$ mice compared with *Jnk1*$^{-/-}$ animals (Fig. 1). This trend was not observed in muscle tissue. Under these conditions, there was no regulation of *Jnk1* or *Jnk2* expression in liver tissue that might explain the difference in kinase activity (data not shown).

Generation of Mice with Combined *Jnk1* and *Jnk2* Mutant Alleles. To address the potential interaction of JNK1 and JNK2 isoforms in obesity and insulin resistance genetically, we intercrossed *Jnk1*$^{-/-}$ and *Jnk2*$^{-/-}$ mice and examined all resultant genotypes under regular and high-fat diet. As reported before, no *Jnk1*$^{-/-}$*Jnk2*$^{-/-}$ double homozygous mutant mice were obtained. Interestingly, in the C57BL/6J background, we also observed a striking reduction in the viability of *Jnk1*$^{-/-}$*Jnk2*$^{+/-}$ animals. Our intercross produced only one mouse of this genotype of >100 pups. At 3 weeks of age, mice were placed on high-fat (50% of the total calories in the form of fat) and high-caloric (5,286 kcal/kg, Bioserve, Frenchtown, NJ) diet along with a control group in each available genotype on a standard diet and were followed for the next 4 months. The growth curves of mice are shown in Fig. 2. Among all seven

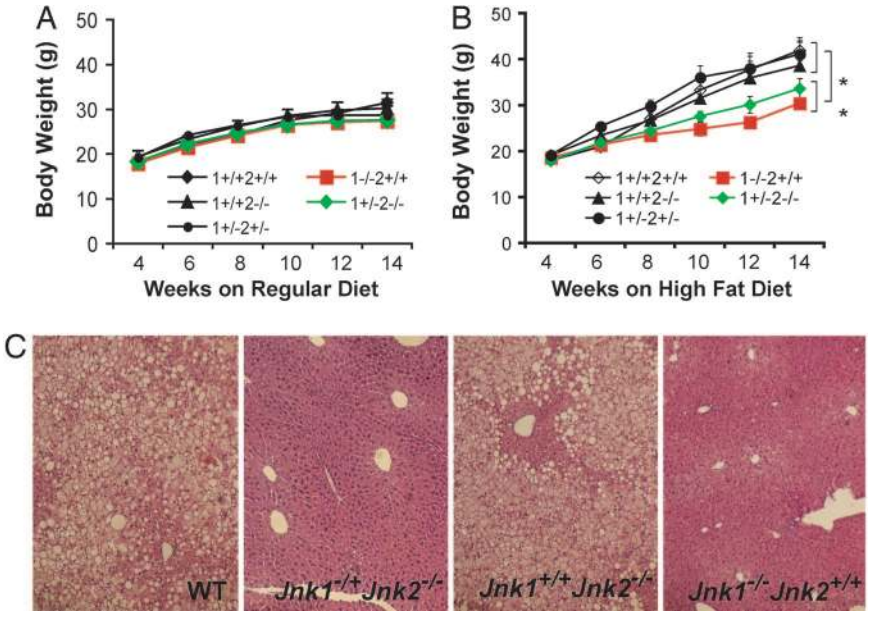

Fig. 2. Body-weight regulation and fatty liver in different *Jnk* genotypes on a high-fat diet. (*A* and *B*) Starting at 3 weeks of age, all progeny from the intercrosses between *Jnk1*$^{+/-}$ and *Jnk2*$^{+/-}$ were placed on a regular (*A*) and high-fat (*B*) diet and were monitored for their body weight. Five genotypes are shown in these graphs. **, statistical significance $P < 0.01$. (*C*) Liver sections prepared from *Jnk1*$^{+/+}$*Jnk2*$^{+/+}$, *Jnk1*$^{+/-}$*Jnk2*$^{-/-}$, *Jnk1*$^{+/+}$*Jnk2*$^{-/-}$, and *Jnk1*$^{-/-}$*Jnk2*$^{+/+}$ mice on with a high-fat/high-caloric diet for 17 weeks. Sections were photographed at ×100 after staining with hematoxylin/eosin.

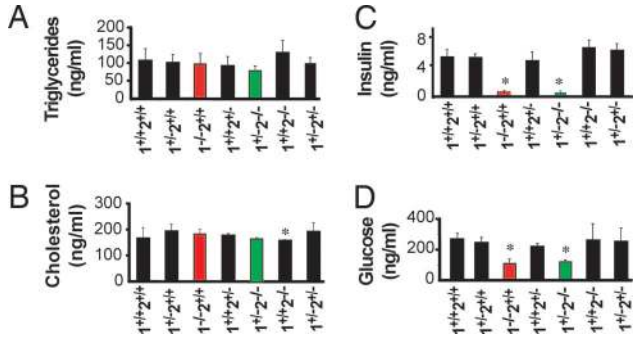

Fig. 3. Biochemical analyses of serum in different *Jnk* genotypes. Serum samples were collected after an overnight fast from mice of the indicated genotypes after 14 weeks on a high-fat diet. Triglyceride (*A*), cholesterol (*B*), insulin (*C*), and glucose (*D*) levels were measured. *, statistical significance $P < 0.05$.

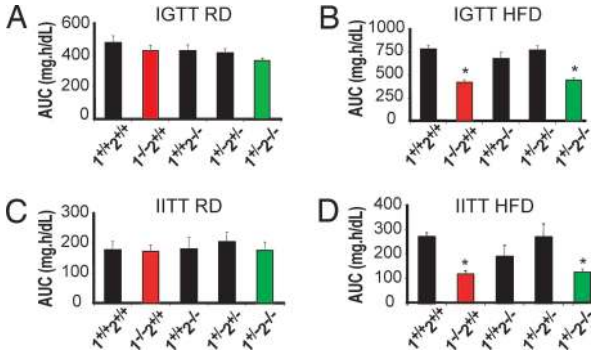

Fig. 4. Comparison of insulin sensitivity among different *Jnk* genotypes. Systemic glucose metabolism and insulin sensitivity were studied by i.p. glucose and i.p. insulin tolerance tests performed on mice kept on a regular (*A* and *C*) and high-fat diet (*B* and *D*) at 16–17 weeks of age. AUC, area under the curve. *, statistical significance $P < 0.01$.

genotypes examined, only $Jnk1^{-/-}Jnk2^{+/+}$ and $Jnk1^{+/-}Jnk2^{-/-}$ mice differed from the rest with respect to their growth curves, where both gained less weight, especially on a high-fat diet, compared with $Jnk1^{+/+}Jnk2^{-/-}$ and $Jnk1^{+/+}Jnk2^{+/+}$ animals (Fig. 2 *A* and *B*). The growth curves of $Jnk1^{+/+}Jnk2^{+/-}$, $Jnk1^{\pm}Jnk2^{+/+}$, and $Jnk1^{+/-}Jnk2^{+/-}$ mice were also indistinguishable from WT animals on either diet (Fig. 2 *A* and *B* and data not shown).

We also examined liver sections prepared from $Jnk1^{+/+}$ $Jnk2^{+/+}$, $Jnk1^{+/-}Jnk2^{-/-}$, $Jnk1^{+/+}Jnk2^{-/-}$, and $Jnk1^{-/-}Jnk2^{+/+}$ mice to determine lipid accumulation and morphology of liver. Although $Jnk1^{+/+}Jnk2^{+/+}$ and $Jnk1^{+/+}Jnk2^{-/-}$ mice fed with a high-fat/high-caloric diet had apparent fatty liver, there was essentially no sign of fatty infiltration in $Jnk1^{-/+}Jnk2^{-/-}$ and $Jnk1^{-/-}Jnk2^{+/+}$animals (Fig. 2*C*).

Plasma Lipids, Glucose, and Insulin Levels in Mutant Mice. In all genotypes, we also determined plasma triglyceride, cholesterol, free fatty acid, and glycerol levels on both regular and high-fat diets. No difference between genotypes was evident with a regular diet (data not shown). These parameters were not different between genotypes on a high-fat diet for 4 months except for a small but statistically significant reduction in blood cholesterol and glycerol levels in $Jnk1^{+/+}Jnk2^{-/-}$ mice on a high-fat diet (Fig. 3 *A* and *B* and data not shown). These results demonstrate that JNK deficiencies had only a minor effect on steady-state lipid homeostasis, as measured by these variables, in the high-fat-diet-induced model of obesity. We also determined plasma insulin and glucose levels in mice that were kept on a high-fat diet for 4 months. Interestingly, all genotypes except for $Jnk1^{-/-}Jnk2^{+/+}$ and $Jnk1^{+/-}Jnk2^{-/-}$ developed significant hyperinsulinemia (Fig. 3*C*). Plasma insulin levels in $Jnk1^{+/+}$ $Jnk2^{-/-}$, $Jnk1^{+/+}Jnk2^{+/+}$, $Jnk1^{+/+}Jnk2^{+/-}$, $Jnk1^{+/-}$ $Jnk2^{+/+}$, and $Jnk1^{+/-}Jnk2^{+/-}$ mice were significantly higher than the levels detected in $Jnk1^{-/-}Jnk2^{+/+}$ and $Jnk1^{+/-}Jnk2^{-/-}$ animals. Similarly, plasma glucose levels were significantly elevated in all genotypes except $Jnk1^{-/-}Jnk2^{+/+}$ and $Jnk1^{+/-}Jnk2^{-/-}$ mice (Fig. 3*D*). Plasma glucose levels in $Jnk1^{+/+}Jnk2^{-/-}$, $Jnk1^{+/+}Jnk2^{+/+}$, $Jnk1^{+/+}Jnk2^{+/-}$, $Jnk1^{+/-}Jnk2^{+/+}$, and $Jnk1^{+/-}Jnk2^{+/-}$ were all significantly higher than the levels detected in $Jnk1^{-/-}Jnk2^{+/+}$ and $Jnk1^{+/-}Jnk2^{-/-}$ animals. These results indicate that *Jnk1* haploinsufficiency renders *Jnk2*-deficient animals resistant to high-fat-diet-induced hyperinsulinemia and hyperglycemia, indicative of systemic insulin resistance.

Systemic Insulin Sensitivity in Mutant Mice. To further investigate systemic glucose metabolism and insulin sensitivity, we performed i.p. insulin and i.p. glucose tolerance tests (Fig. 4). In both tests, mice kept on regular diet behaved the same regardless of their genotype (Fig. 4 *A* and *C*), whereas in mice fed the high-fat diet, $Jnk1^{-/-}Jnk2^{+/+}$ and $Jnk1^{+/-}Jnk2^{-/-}$ mice showed improved glucose metabolism and systemic insulin sensitivity compared with other genotypes (Fig. 4 *B* and *D*).

The i.p. glucose tolerance test performed on mice fed a high-fat diet demonstrated that the glucose disposal curves of $Jnk1^{-/-}$ $Jnk2^{+/+}$ and $Jnk1^{+/-}Jnk2^{-/-}$ animals were comparable to each other but different from the other genotypes tested, and the area under the curve showed a statistically significant difference in these mice compared with $Jnk1^{+/+}Jnk2^{+/+}$, $Jnk1^{+/-}Jnk2^{+/-}$, and $Jnk1^{+/+}Jnk2^{-/-}$ animals (Fig. 4*B*). Similarly, in the i.p. insulin tolerance test, the $Jnk1^{-/-}Jnk2^{+/+}$ and $Jnk1^{+/-}Jnk2^{-/-}$ groups differed from the other genotypes (Fig. 4*D*). The area under the curve revealed a statistically significant difference in the hypoglycemic responses of both $Jnk1^{-/-}Jnk2^{+/+}$ and $Jnk1^{+/-}Jnk2^{-/-}$ mice compared with all other genotypes examined. Hence, deleting one *Jnk1* allele rendered $Jnk1^{+/+}Jnk2^{-/-}$ animals that otherwise develop insulin resistance on a high-fat diet (10) refractory to diet-induced metabolic deterioration.

JNK Activity and Inflammatory Cytokine Expression in Mutant Mice. We next determined whether JNK activity and, more importantly, cytokine expression patterns differ between $Jnk1^{+/-}$ $Jnk2^{-/-}$ animals and those observed in $Jnk1^{+/+}Jnk2^{-/-}$ mice. As shown in Fig. 5*A*, the metabolic stress induced by obesity increases JNK kinase activity, which has been ascribed primarily to that of the JNK1 isoforms (10). Here, we compared JNK activity in livers of $Jnk1^{-/-}Jnk2^{+/+}$, $Jnk1^{+/+}Jnk2^{-/-}$, and $Jnk1^{+/-}Jnk2^{-/-}$ animals on a high-fat diet where the compensatory changes are most apparent. As expected, $Jnk1^{-/-}$ $Jnk2^{+/+}$ mice had barely detectable JNK activity in liver tissue, whereas $Jnk1^{+/+}Jnk2^{-/-}$ animals exhibited significantly higher levels of total JNK activation with the high-fat diet. However, in $Jnk1^{+/-}Jnk2^{-/-}$ mice, total liver JNK activity was significantly reduced to levels similar to those seen in lean mice (Fig. 5*A*). These data indicate that elevated JNK activity observed in $Jnk1^{+/+}Jnk2^{-/-}$ mice is derived from JNK1 isoforms, whose liver tissue expression in the $Jnk1^{+/-}$ background is reduced by 50% (data not shown).

It is now well established that obesity triggers low-grade inflammation (1), and JNK is likely to be one of several protein kinases that play a role in this response and in inflammatory cytokine production in insulin-sensitive sites (28). We therefore examined the expression levels of mRNAs for several proinflammatory cytokines, which are expected to be regulated through the JNK-AP-1 pathway, using liver samples from

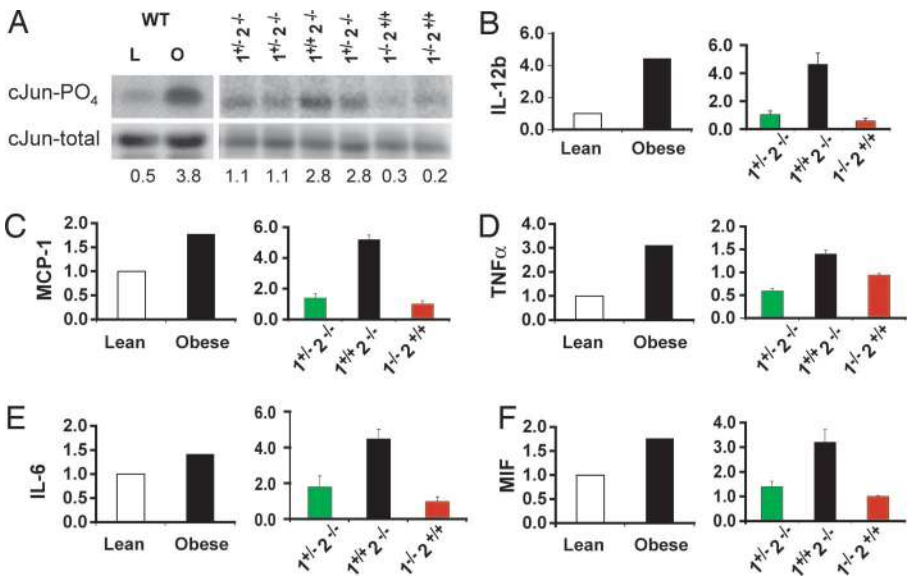

Fig. 5. Total JNK activity and expression of inflammatory cytokines. Total JNK activity was determined in livers of $Jnk1^{+/-}Jnk2^{-/-}$, $Jnk1^{-/-}Jnk2^{+/+}$, and $Jnk1^{+/+}Jnk2^{-/-}$ mice kept on a high-fat diet (*A*) along with their lean and obese WT controls at 17 weeks of age. Total RNA was extracted from the same liver samples, and IL-12 (*B*), MCP-1 (*C*), TNF-α (*D*), IL-6 (*E*), and MIF (*F*) mNA levels were quantified relative to that of 18S ribosomal RNA.

$Jnk1^{+/-}Jnk2^{-/-}$, $Jnk1^{+/+}Jnk2^{-/-}$, and $Jnk1^{-/-}Jnk2^{+/+}$ mice fed a high-fat diet along with lean and obese WT mice. These included the mRNAs for: TNF-α, IL-6, IL-12, monocyte chemotactic protein 1 (MCP-1), and macrophage migration inhibitory factor (MIF). In obese WT animals, expression levels of these cytokines in liver tissue were higher than in lean controls (Fig. 5 *B–F*). Interestingly, $Jnk1^{+/+}Jnk2^{-/-}$ mice on a high-fat diet exhibited the highest levels of inflammatory cytokine expression among all genotypes examined. In contrast, the abundance of TNF-α, IL-6, IL-12, MCP-1, and MIF mRNAs was significantly reduced in $Jnk1^{-/-}Jnk2^{+/+}$ as well as $Jnk1^{+/-}Jnk2^{-/-}$ mice, to levels seen in WT lean mice. Hence, the balance between JNK1 and JNK2 isoform expression, which influences total JNK activity, is a critical determinant of inflammatory cytokine production in obesity.

Obesity is associated with a marked increase in JNK activity at insulin-sensitive sites. In our earlier work, we ascribed this activity predominantly to JNK1 isoforms, because disruption of the *Jnk1* locus prevented the obesity-related increase in JNK activity (10). Consistent with this observation, there is also recovery from impaired insulin receptor signaling, fatty liver and systemic insulin resistance in $Jnk1^{-/-}$ mice on a high-fat diet, along with reduced total body adiposity (10). Because none of these alterations were apparent in $Jnk2^{-/-}$ mice, initially these observations ruled out a possible role, either negative or positive, for JNK2 in obesity and diabetes. However, subsequent experiments with $Jnk2^{-/-}$ animals revealed an increase in total JNK activity, particularly in the liver. This activity is reduced upon removal of one *Jnk1* allele, which also reduces *Jnk1* expression by half. Thus, the balance between JNK1 and JNK2 isoform expression levels is an important determinant of total JNK activity in fat-laden tissues, such as the liver.

In fact, the existence of such cross-regulatory interactions between JNK1 and JNK2 isoforms was recently demonstrated in the context of cell proliferation (27). In this example, the interaction of JNK1 and JNK2 with c-Jun is differentially regulated under baseline and stimulated conditions and results in c-Jun phosphorylation with or without degradation (27). Additional studies should illustrate whether a similar mechanism is also in play in the context of metabolic regulation. It is likely that other pathways are also involved, because not only cytokine expression, which may be affected by c-Jun N-terminal phosphorylation (29), but also total JNK activity, insulin sensitivity, and hepatic lipid accumulation are modulated upon exposure to dietary obesity in *Jnk2*-deficient animals. All are reversed in $Jnk2^{-/-}$ mice by introducing *Jnk1* haploinsufficiency, which alone has no effect on the metabolic phenotype of mice under regular or high-fat diet. Indeed, insulin sensitivity is directly regulated, at least in part through Ser-307 phosphorylation of IRS-1 rather than c-Jun N-terminal phosphorylation (10). Of note, *in vitro* JNK1 and JNK2 exhibit similar affinity and activity toward IRS-1 (Fig. 6). Hence, the most critical determinant of insulin sensitivity, fat-induced cytokine expression, and even overall weight gain appears to be total JNK kinase activity, which is a function of the balance of JNK1 and JNK2 isoform expression.

Notably, whereas isolated *Jnk2* deficiency had no impact on diet-induced obesity and insulin resistance, it protected animals against type 1 diabetes and atherosclerosis (25, 26). We observed a small but statistically significant reduction in plasma cholesterol, which may contribute to the atheroprotective effect of JNK2 deficiency. It is possible that a similar role for JNK1 may exist in this context, which will not be apparent in isolated JNK isoform deficiency models. Although these pathologies might reflect an absolute JNK isoforms dependence, they raise an interesting possibility that the phenotypic impact of a deficiency in a given JNK isoform might in fact be a reflection of compensatory changes of different metabolic responses to total JNK activity. For instance, elevated JNK activity under certain circumstances may exert an antiapoptotic or protective effect (30), whereas in the context of an IκB kinase (IKK) deficiency and a high level of TNF-α, it is a critical mediator of apoptosis (23). Even the interaction between IKK deficiency and JNK activity is context-specific and not observed in obesity (data not shown).

These results indicate the importance of the interplay between JNK1 and JNK2 isoforms in the regulation of lipid and glucose metabolism in the whole organism. Because JNK inhibitors are widely pursued for the treatment of metabolic as well as other inflammatory diseases, consideration of isoform-specific interventions should take into account the compensatory changes in JNK activity that may be caused by differential inhibition of JNK1 and JNK2 isoforms.

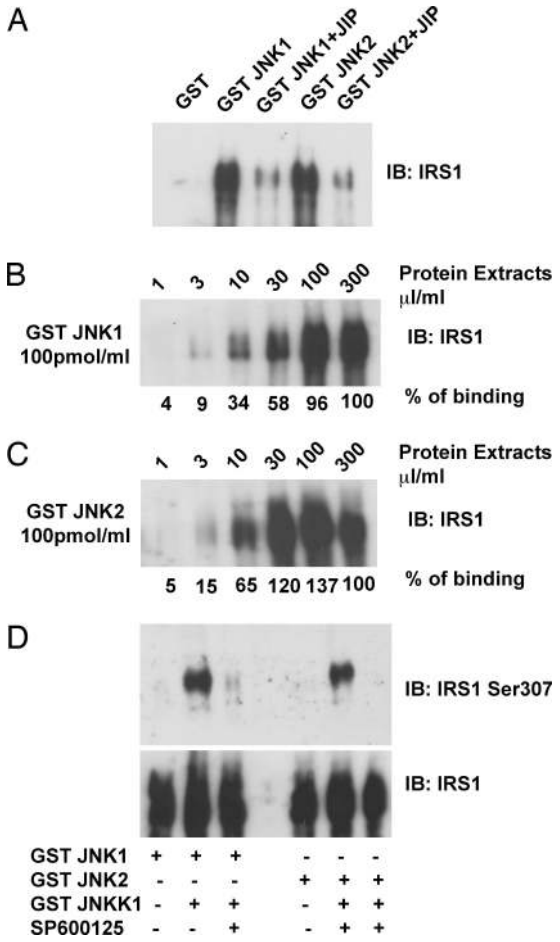

Fig. 6. Binding of JNK1 and JNK2 to IRS-1 and its phosphorylation on Ser-307 residue. (*A*) GST pulldown of lysates (300 μg/ml) from HEK293T cells transiently expressing IRS-1 in the presence or absence of the competitive inhibitor of JNK substrate docking, Tat-JIP (5 μM). (*B* and *C*) GST-JNK1 (*B*) and GST-JNK2 (*C*) pulldown experiments using different amounts of extracts from IRS-1-expressing HEK293T cells. (*D*) GST-JNK1 and GST-JNK2 pulldown kinase assays were performed by using 300 μg/ml of protein lysates from IRS-1-expressing HEK293T cells in the presence or absence of the JNK inhibitor SP600125 (2 μM). IRS-1 Ser-307 phosphorylation was detected by immunoblotting with a phosphospecific antibody.

Methods

Generation of Mice Deficient in JNK1 and JNK2. *Jnk1*$^{-/-}$ and *Jnk2*$^{-/-}$ mice were described elsewhere (18, 21). *Jnk1*$^{-/-}$ mice were initially on a C57BL/6/129 mixed genetic background but, before setting up the colony, they were backcrossed for three generations to C57BL/6. *Jnk1*$^{-/-}$ mice were then intercrossed with *Jnk2*$^{-/-}$ mice on a C57BL/6 background (two more backcrosses) to produce *Jnk1*$^{+/-}$*Jnk2*$^{+/-}$ and *Jnk1*$^{+/-}$*Jnk2*$^{-/-}$ mice. All experimental mice were generated from intercrosses between double heterozygous animals, and experimental groups were formed by using littermates.

Diet Study and Metabolic Measurements. Male mice with mutations at the *Jnk1* and/or *Jnk2* loci and their WT littermates were housed in a pathogen-free facility and placed on a high-fat/high-calorie diet (50% of the total calories in the form of fat, 5,286 kcal/kg, Diet F3282; Bioserve) ad libitum at 3 weeks of age and were followed for a period of 16 weeks. Parallel groups of animals were left on standard rodent chow to serve as controls. Body-weight measurements were taken starting at 4 weeks of age. Blood samples were collected after a 6-h daytime fast at indicated ages. Serum glucose, insulin, triglyceride, and free fatty acid levels were measured as described (10). Glucose and insulin tolerance tests were performed on conscious mice after a 6-h fast (3). Glucose tolerance tests were done by i.p. administration of glucose (1.8 g/kg) and measurement of blood glucose at $t = 15$, 30, 60, 90, and 120 min in 16-week-old mice. Insulin tolerance tests were done similarly except for the injection of human insulin (1 unit per kg; Lilly Research Laboratories, Indianapolis). LPS (Sigma) was administered i.p. at a dose of 100 mg/kg. The mice were killed and the tissues harvested 2 h after injection.

The animal numbers in each of the experiments ranged between 4 and 11, except for the gene expression studies, which were conducted in two animals for each genotype in each experiment.

Measurement of JNK Activity and Protein Levels. Tissue lysates containing 600 μg of protein were mixed with 20 μl of GST-agarose resin suspension (Sigma), to which 5 μg of GST-c-Jun (1–79) was bound. The mixture was agitated at 4°C overnight, pelleted by centrifugation, and washed twice in buffer containing 20 mM Hepes, pH 7.7/50 mM NaCl/2.5 mM $MgCl_2$/0.5 mM EDTA and once with JNK assay buffer. The pelleted beads were subjected to *in vitro* kinase assay by using standard conditions (31). The bands corresponding to GST-c-Jun were quantified by using PhosphorImager.

Real-Time RT-PCR. Total RNA was isolated from 50-mg liver tissue samples by using TRIzol reagent (Invitrogen). The reverse-transcription reaction was carried out with the ThermoScript RT-PCR system (Invitrogen). Real-time PCR analysis was performed in a 25-μl final volume with an iCycler iQ Detection System by using iQ SYBR Green Supermix (Bio-Rad). The PCR thermal cycling program was: 2 min 30 s at 95°C, 40 cycles of 15 s at 95°C, 30 s at 58°C, and 1 min at 72°C for extension. Real-time PCR products were confirmed by melting curve analysis. Quantitations were normalized to the 18S rRNA level in each reaction. Primer sequences were: 18S forward, AGTCCCTGCCCTTTGTACACA; 18S reverse, CGATCCGAGGGCCTCACTA; IL-6 forward, ACAACCACGGCCTTCCCTACTT; IL-6 reverse, CACGATTTCCCA GAGAACATGTG; MCP-1 forward; CCACTCACCTGCTGCTACTCAT; MCP-1 reverse, TGGTGATCCTCTTGTAGCTCTCC; MIF forward, GCCAGAGGGGTTTCTGTCG; MIF reverse, GTTCGTGCCGCTAAAAGTCA; TNF-α forward, CCCTCACACT CAGA TCATCTTCT; TNF-α reverse, GCTACGACGTGGGCTACAG; IL-12b forward, AGACAT GGAGTCATAGGCTCTG; and IL-12b reverse, CCATTTTCCTTCTTGTGGAGCA.

JNK1 and JNK2 Binding and Phosphorylation of IRS-1. For GST pulldown, 100 pmol of GST, GST-JNK1, or GST-JNK2 was incubated for 2 h at 4°C with 300 μg of lysates from HEK293T cells transfected with pcDNA3IRS-1 in 1 ml of lysis buffer in the presence or absence of a synthetic peptide corresponding to the D-domain of JNK-interacting protein. The beads were washed three times with lysis buffer, and IRS-1 binding was detected by immunoblot by using a specific IRS-1 antibody (Upstate Biotechnology, Lake Placid, NY). To compare the ability of JNK1 and JNK2 to phosphorylate IRS-1 at Ser-307, pulldown was performed as described above by using 300 μg of protein extracts. Beads were washed twice in lysis buffer (20 mM Tris, pH 7.5/150 mM NaCl/1 mM EDTA/1% Triton X-100) and once in kinase buffer (25 mM Tris·HCl, pH 7.5/10 mM $MgCl_2$). The kinase reaction was initiated by addition of ATP (300 μM) and the upstream kinase JNKK1 (2 pmol). IRS-1 Ser-307 phosphorylation was detected by immunoblot by using Ser-307-phosphospecific antibody (Upstate Biotechnology). As loading control, the membranes were analyzed

with antibody against total IRS-1 (Upstate Biotechnology). pcDNA3-IRS-1 used to transiently express IRS-1 in HEK293T cells was provided by Luciano Pirola (University of Lyon, Lyon, France).

This work was supported in part by National Institutes of Health Grants DK52539 (to G.S.H.) and ES04151 (to M.K.) and an American Diabetes Association Mentor Award (to M.K.). G.T. was supported by a postdoctoral fellowship from the Iacocca Foundation.

1. Wellen, K. E. & Hotamisligil, G. S. (2005) *J. Clin. Invest.* **115,** 1111–1119.
2. Hotamisligil, G. S., Shargill, N. S. & Spiegelman, B. M. (1993) *Science* **259,** 87–91.
3. Uysal, K. T., Wiesbrock, S. M., Marino, M. W. & Hotamisligil, G. S. (1997) *Nature* **389,** 610–614.
4. Ventre, J., Doebber, T., Wu, M., Macnaul, K., Stevens, K., Pasparakis, M., Kollias, G. & Moller, D. E. (1997) *Diabetes* **46,** 1526–1531.
5. Shulman, G. I. (2000) *J. Clin. Invest.* **106,** 171–176.
6. Boden, G. (1997) *Diabetes* **46,** 3–10.
7. Kanety, H., Feinstein, R., Papa, M. Z., Hemi, R. & Karasik, A. (1995) *J. Biol. Chem.* **270,** 23780–23784.
8. Hotamisligil, G. S., Peraldi, P., Budavari, A., Ellis, R., White, M. F. & Spiegelman, B. M. (1996) *Science* **271,** 665–668.
9. Yuan, M., Konstantopoulos, N., Lee, J., Hansen, L., Li, Z. W., Karin, M. & Shoelson, S. E. (2001) *Science* **293,** 1673–1677.
10. Hirosumi, J., Tuncman, G., Chang, L., Gorgun, C. Z., Uysal, K. T., Maeda, K., Karin, M. & Hotamisligil, G. S. (2002) *Nature* **420,** 333–336.
11. Kaneto, H., Nakatani, Y., Miyatsuka, T., Kawamori, D., Matsuoka, T. A., Matsuhisa, M., Kajimoto, Y., Ichijo, H., Yamasaki, Y. & Hori, M. (2004) *Nat. Med.* **10,** 1128–1132.
12. Aguirre, V., Uchida, T., Yenush, L., Davis, R. & White, M. F. (2000) *J. Biol. Chem.* **275,** 9047–9054.
13. Ozcan, U., Cao, Q., Yilmaz, E., Lee, A. H., Iwakoshi, N. N., Ozdelen, E., Tuncman, G., Gorgun, C., Glimcher, L. H. & Hotamisligil, G. S. (2004) *Science* **306,** 457–461.
14. Emanuelli, B., Peraldi, P., Filloux, C., Chavey, C., Freidinger, K., Hilton, D. J., Hotamisligil, G. S. & Van Obberghen, E. (2001) *J. Biol. Chem.* **276,** 47944–47949.
15. Nguyen, M. T., Satoh, H., Favelyukis, S., Babendure, J. L., Imamura, T., Sbodio, J. I., Zalevsky, J., Dahiyat, B. I., Chi, N. W. & Olefsky, J. M. (2005) *J. Biol. Chem.* **280,** 35361–35371.
16. Davis, R. J. (2000) *Cell* **103,** 239–252.
17. Karin, M. & Gallagher, E. (2005) *IUBMB Life* **57,** 283–295.
18. Sabapathy, K., Hu, Y., Kallunki, T., Schreiber, M., David, J. P., Jochum, W., Wagner, E. F. & Karin, M. (1999) *Curr. Biol.* **9,** 116–125.
19. Dong, C., Yang, D. D., Wysk, M., Whitmarsh, A. J., Davis, R. J. & Flavell, R. A. (1998) *Science* **282,** 2092–2095.
20. Yang, D. D., Conze, D., Whitmarsh, A. J., Barrett, T., Davis, R. J., Rincon, M. & Flavell, R. A. (1998) *Immunity* **9,** 575–585.
21. Sabapathy, K., Kallunki, T., David, J. P., Graef, I., Karin, M. & Wagner, E. F. (2001) *J. Exp. Med.* **193,** 317–328.
22. Gao, M., Labuda, T., Xia, Y., Gallagher, E., Fang, D., Liu, Y. C. & Karin, M. (2004) *Science* **306,** 271–275.
23. Chang, L., Kamata, H., Solinas, G., Luo, J. L., Maeda, S., Venuprasad, K., Liu, Y. C. & Karin, M. (2006) *Cell* **124,** 601–613.
24. Liu, J., Minemoto, Y. & Lin, A. (2004) *Mol. Cell. Biol.* **24,** 10844–10856.
25. Ricci, R., Sumara, G., Sumara, I., Rozenberg, I., Kurrer, M., Akhmedov, A., Hersberger, M., Eriksson, U., Eberli, F. R., Becher, B., *et al.* (2004) *Science* **306,** 1558–1561.
26. Jaeschke, A., Rincon, M., Doran, B., Reilly, J., Neuberg, D., Greiner, D. L., Shultz, L. D., Rossini, A. A., Flavell, R. A. & Davis, R. J. (2005) *Proc. Natl. Acad. Sci. USA* **102,** 6931–6935.
27. Sabapathy, K., Hochedlinger, K., Nam, S. Y., Bauer, A., Karin, M. & Wagner, E. F. (2004) *Mol. Cell* **15,** 713–725.
28. Hotamisligil, G. S. (2005) *Diabetes* **54,** Suppl. 2, S73–S78.
29. Karin, M. (1995) *J. Biol. Chem.* **270,** 16483–16486.
30. Ventura, J. J., Cogswell, P., Flavell, R. A., Baldwin, A. S., Jr. & Davis, R. J. (2004) *Genes Dev.* **18,** 2905–2915.
31. Hibi, M., Lin, A., Smeal, T., Minden, A. & Karin, M. (1993) *Genes Dev.* **7,** 2135–2148.